Ingeniería Investigación y Tecnología, volumen XVI (número 4), octubre-diciembre 2015: 491-501
ISSN 2594-0732 FI-UNAM
(artículo arbitrado)
DOI: https://doi.org/10.1016/j.riit.2015.09.002

Influence of Chemically Treated Palygorskite Over the Rheological Behavior of Polypropylene Nanocomposites

Influencia de paligorskita químicamente tratada sobre el comportamiento reológico de nanomateriales compuestos de polipropileno

Soberanis-Monforte Genaro Antonio
Unidad de Materiales
Centro de Investigación Científica de Yucatán, AC
E-mail: genaro.soberanis@cicy.mx

Gordillo-Rubio José Luis
Unidad de Materiales
Centro de Investigación Científica de Yucatán, AC
E-mail: jose29011982@yahoo.com.mx

González-Chi Pedro Iván
Unidad de Materiales
Centro de Investigación Científica de Yucatán, AC
E- mail: ivan@cicy.mx
Autor para correspondencia

Information on the article: received: March 2014, reevaluated: June 2014, accepted: February 2015

Abstract

Melt compounding was used to prepare thermoplastic composites reinforced with palygorskite; the chemical modification of the palygorskite surface and the control of extrusion parameters were used to promote good dispersion and a good interface with the matrix, affecting the rheological properties of the mixture, since the melt viscoelastic behavior is sensitive to changes in the molecular structures at nanoscale and mesoscale. The palygorskite nanoclay (diameter 30 nm) was extracted from a site in the southeast of the state of Yucatan, Mexico; the palygorskite was subjected to purification and then superficially modified with 3-aminopropyltrimetoxysilane. These processes generated three types of specimens: unpurified, purified and purified-silanized palygorskite; which were subsequently incorporated (0.5 w%) to a polypropylene matrix by twin extrusion. Frequency sweeps were used to evaluate the interaction between the matrix and the nano-reinforcement. The master curves of storage modulus (G′), loss modulus (G″) and complex viscosity (η*) *vs* angular frequency (ω_x) show a change of the interfacial interaction polypropylene/palygorskite when the palygorskite was chemically modified.

Keywords:

- Palygorskite
- morphology
- nanocomposite
- rheology
- Polypropylene

DOI: https://doi.org/10.1016/j.riit.2015.09.002

Resumen

El método de mezclado en fundido se utilizó para preparar materiales compuestos termoplásticos reforzados con paligorskita; la modificación química de esta y el control de los parámetros de extrusión se usaron para promover una buena dispersión y buena interface con la matriz polimérica, afectando las propiedades reológicas de la mezcla, ya que el comportamiento viscoelástico en fundido es sensible a los cambios en las estructuras moleculares tanto a nanoescala como a mesoescala. La nanoarcilla paligorskita se extrajo de una mina a cielo abierto situada en el sureste del estado de Yucatán, México; esta arcilla fue sometida a un proceso de purificación y una modificación superficial con 3-aminopropiltrimetoxisilano. Estos procesos generaron tres tipos de especímenes: paligorskita sin purificar, purificada y purificada-silanizada; las cuales fueron incorporadas (0.5 w%) a una matriz de polipropileno por extrusión de doble husillo. Barridos de frecuencia se emplearon para evaluar la interacción entre la matriz y el nano-refuerzo. Las curvas maestras del módulo de almacenamiento (G'), módulo de pérdida (G") y la viscosidad compleja (η) vs la frecuencia angular (ω_x) mostraron un cambio en la interacción interfacial polipropileno/ paligorskita cuando la arcilla se modificó químicamente.*

Descriptores:

- *Paligorskita*
- *morfología*
- *nanomateriales compuestos*
- *reología*
- *Polipropileno*

Introduction

The basic structure of fibrous palygorskite was proposed by Bradley in 1940: $[Si_8Mg_5O_{20}(OH)_2](H_2O)_4 \cdot 4H_2O$; the water molecules associated with the palygorskite structure show three different linkages: hygroscopic water, coordinated water and structural water. Palygorskite is widely used in different applications such as animal waste adsorbent, pesticide carrier, decolorizing agent, catalyst and catalyst support and as excipient for medical drugs (Dos Santos, 2013).

The adsorbent and catalytic applications of the palygorskite depend from the surface physico-chemical properties, which can be modified by chemical and thermal treatments to control the surface activity (Jimenez *et al*., 1978; Bonilla *et al*., 1981; Pesquera *et al*., 1992; Duan *et al*., 2011). Although palygorskite has been studied from different points of view (Abdul & Weaver, 1969; Corma *et al*., 1987 y 1990; Gonzalez *et al*., 1990), the literature concerning this mineral is less abundant than that for sepiolite or other smectites.

Clays are being used to create new materials with unique characteristics, and among the most interesting are the composites in which the clay is mixed at nano level with a polymer; these materials are known as *polymer-silicate nanocomposites* (PSNs). They only incorporate a small amount of silicates but provide good mechanical, thermal, and barrier properties (Kojima *et al*., 1993; Furuichi *et al*., 1996; Wang *et al*., 2001; Koo *et al*., 2005). One of the real challenges posed by the PSNs is the distribution of nano-reinforcement in the matrix, which may affect the range of applications for PSNs (Chen *et al*., 2010). Depending on the chemical nature of the constituents and the interactions between nanoreinforcing particles, their dispersion can generate agglomerated, intercalated and exfoliated structures (Koo *et al*., 2003).

Molten compounding to disperse the nanoclay in a thermoplastic polymer is a promising technique for manufacturing PSNs, due to its ease of operation (Chen *et al*., 2010), low cost and minimal impact on the environment. This processing method is based on conventional polymer blending by twin screw extrusion. When this processing method is used with non-polar polymers such as *polypropylene* (PP), compatibilizing agents are required because the shear stresses generated during the processing are not sufficient to disperse the nanoclay in the matrix. A generally accepted practice is to add *maleated polypropylene* (MaPP) as a compatibilizer. However, parameters like the molecular weight of the MaPP and the content of grafted *maleic anhydride* (MA) must be taken into account. It has been found that in the case of laminar clays, a high content of MA generally increases the melt intercalation of PP chains in the clay structure which leads to a separation of the clay sheets, however, the presence of the MA can also generate immiscibility with the PP matrix, thus affecting the mechanical properties of the nanocomposites (Kato *et al*., 1997; Koo *et al*., 2003; Ville *et al*., 2012). The influence of the molecular weight is less clear; most authors have used low molecular weight MaPP (Kato *et al*., 1997; Kawasumi *et al*., 1997; Hasegawa *et al*., 1998; Hasegawa, *et* al, 2000), nevertheless, high molecular weight improves the mechanical properties. The presence of MaPP

DOI: https://doi.org/10.1016/j.riit.2015.09.002

with different molecular weights not only affects the final morphology of the nanocomposite but also the melt behavior of the matrix (Reichert *et al*., 2000).

The size, shape, structure and surface characteristics of the disperse phase affect the rheological properties of the molten matrix, often negatively. However, with nanoparticles, the interaction between the reinforcement and the matrix takes place at the molecular level, directly affecting molecular motion and flow. For this reason, the dispersion degree and interfacial interaction between nanoclay and a thermoplastic matrix affects the rheological properties of a nanocomposite, and knowledge of the nanocomposite rheological behavior leads to the optimization of the material processing (extrusion or injection).

A considerable number of studies have been conducted on the mechanical, rheological and thermal properties of PSNs; Ghaffarpour and Khodaii (2009) found that by adding nanoclays to bitumen, the material's rheological properties changed; not only the material stiffness increased, but also the phase angle (δ) decreased and the aging resistance improved. Mahi and Rodrigue (2012) performed dynamic rheological tests using ethylene vinyl acetate/nano-crystalline cellulose composites, at low frequencies, and a pseudo solid-like behavior was observed, which was correlated to particle networks related to the hydrogen bonding between the cellulose molecules. Jin and Zhong (2013) performed dynamic rheological tests to measure the storage (G ') and loss (G '') moduli at different temperatures using soy protein hydrogels reinforced with nanoclays to estimate the cross-linking time of the mixture. Little information has been found related to the influence of nanoclay dispersion on the rheological properties of PSNs (Vaia *et al*., 1997). Hoffmann *et al.* (2000) and Lim and Park (2001) used rheological techniques to establish that the linear viscoelastic properties of nanocomposites are highly affected by the degree of clay dispersion at the polymeric matrix, particularly nanocomposites where the polymer chains and the clay surface are chemically bonded (Krishnamoorti *et al*., 1996; Vaia & Giannelis, 1997). Some other factors should be considered to improve the properties of PSNs; as mentioned by Murray and Zhou (2006), the amount of clay used and the physical properties of palygorskite and sepiolite like particle size, shape, distribution, surface area, chemical charge are a key factor to control the performance of the PSN's, also due to the fibrillar nature of these clays, the fiber length is a parameter to be closely controlled to get high quality materials.

Experimental

Materials

The clay used as reinforcement of the PSNs was palygorskite with an average diameter of 30 nm. Table 1 shows the chemical composition of the palygorskite (Soberanis G) extracted from a quarry located in Ticul, Yucatan, Mexico. The matrix used was isotactic *polypropylene* (PP). The compatibilizer was *maleated polypropylene* (MaPP); Table 2 shows the properties of the PP and MaPP. The palygorskite purification process utilized: hydrogen peroxide at 30% (w/v), glacial acetic

Table 1. Chemical composition of the extracted palygorskite measured by EDAX (Soberanis G)

Element	%
O	52.28
Si	22.40
C	12.24
Mg	5.27
Al	4.21
Fe	2.20
K	0.36
Ca	0.80
Na	0.03
Cl	0.21

Table 2. Physics properties of MaPP and PP

Material	MFI (g/10 min)	M_w	M_n	Acid number (mg KOH/g)	Maleic anhydride (%)	T_m (°C)	Density (g/cm^3)
MaPP Aldrich 426512	115	107814	39417	5.34	0.5	152	0.95
PP Valtec HP423M	3.8	232400	80142	0	0	165	0.9

DOI: https://doi.org/10.1016/j.riit.2015.09.002

acid, hydroxylamine chloride and sodium hexametaphosphate, all of them reagent grade and hydrogen peroxide at 3.95% (w/v) medical grade. For the silanization process, 3-aminopropyltrimethoxysilane was used.

Extraction and purification of the palygorskite

The purification process of the palygorskite consisted of five treatments:

1) 30 g of palygorskite was mixed with 400 mL of distilled water for 3 h until total dispersion, after which the solution was filtered to remove stony debris.

2) 200 mL of hydrogen peroxide at 30% (w/v) was added and stirred until the bubbling ceased and then 300 mL of hydrogen peroxide at 3.95% (w/v) was added. Once the bubbling ended, the solution was heated at 100°C to evaporate the water; the addition of hydrogen peroxide at 3.95% (w/v) was repeated until no color change was observed in the solution. 3 mL of glacial acetic acid was added and the solution was evaporated; finally, the palygorskite was dried in an oven for 8 h at 100°C.

3) 240 mL of a solution 1 M of sodium acetate adjusted to pH 5 and 300 mL of distilled water were added to the palygorskite and stirred for 3 h. The mixture was then centrifuged at 1500 rpm for 15 min periods, and the sediments were decanted and dried in an oven at 100°C for 8 h.

4) 450 mL of hydroxylamine chloride 0.04 M and 150 mL of glacial acetic acid were added to the palygorskite and the mixture was heated at 96 ± 3°C with occasional stirring for 6 h; 600 mL of distilled water was added to the palygorskite and stirred and evaporated for 30 min after which the mixture was centrifuged at 1500 rpm during 15 min periods; the palygorskite was washed until the liquid fraction was colorless and odorless; finally, the palygorskite was dried in an oven at 100°C for 8 h (Tessier *et al*., 1979).

5) 1000 mL of the dispersant solution of sodium hexametaphosphate at 0.5% (w/v) was added to the palygorskite and stirred for 8 h, after which the solution was placed for 60 min in an ultrasonic bath, and centrifuged at 2000 rpm for 60 min; it was then decanted and the palygorskite was dried in a vacuum oven at 80°C at -635 mm Hg. Finally, the palygorskite was grinded and stored.

Silanization process of the purified palygorskite

Silanization of the palygorskite was performed using the following methodology: 500 mL of distilled water was added to 10 g of purified palygorskite and sonicated for 1 min; the solution was heated to a temperature between 40 and 45°C and stirred for 10 min. 2.5 mL of 3-aminopropyltrimethoxysilane was added drop by drop for 60 min; the mixture was then centrifuged at 2000 rpm for 20 min and decanted. 25 mL of ethanol was added to each centrifuge tube and these were placed in an ultrasonic bath for 10 min, after which 25 mL of distilled water was added to each tube and centrifuged at 2000 rpm for 10 min extra. 40 mL of distilled water was added to each centrifuge tube which were then sonicated for 10 min and centrifuged for 10 min at 2000 rpm. The solid material in the centrifuge tubes was dried in a vacuum oven at 80°C at -635 mm Hg. Finally, the palygorskite was grinded and stored.

Infrared spectroscopy

3 mg of palygorskite were mixed with 130 mg of KBr and the mixture was subjected to a pressure of 10 ton in a Carver hydraulic press to mold a tablet that was dried in a vacuum oven at -635 mm Hg and 100ºC for 24 h. The spectrophotometer used was a Fourier Transform Infrared (FTIR) Nicolet model Protege 460. The spectra were obtained in the range from 4000 to 400 cm^{-1} with a resolution of 4 cm^{-1} and 100 scans.

Scanning electron microscopy

Microscopic examination was performed to establish the morphology of the palygorskite before and after each one of the treatments from the purification process. The scanning electron microscope (SEM) used was a JEOL model JSM-6360-LV. The scans were performed with 20 kV in high vacuum mode with magnifications of 10,000x and 20,000x. The samples were coated with gold in a Denton Vacuum Desk-II cold sputtering machine, with a deposition time of 18 s.

Extrusion and molding of the PSN's

The PP/nanoclay blends were prepared in a twin-screw extruder with three heating zones (model CTSE-V/MARK-II, Brabender) equipped with a drive unit Plasticorder (model 813402). The length of the screw is 400 mm with an L/D ratio of 13:1. The extrusion conditions used were the speed of the spindle at 150 rpm and the temperature of the heating zones and die, 180, 200, 210

DOI: https://doi.org/10.1016/j.riit.2015.09.002

and 210°C, respectively. The extruder was fed with three dispensers calibrated to generate the formula: 0.5 wt% palygorskite, 10 wt% MaPP and 89.5 wt% PP. The extrudates were molded into sheets of 150 x 150 x 0.9 mm in a Carver semiautomatic press at 210°C with a progressive compression force of 4500 kgf.

Rheometric frequency sweeps

The rheological analysis was performed in a rheometer TA instrument, model AR-2000 fitted with parallel plates of 25 mm of diameter. The frequency sweep experiments were performed on specimen disks with an average 25 mm diameter and 0.9 mm thickness; a pneumatic pressure of 2.07 Bar and 10% strain was used, the test temperatures in the environmental chamber of the rheometer were 170, 190 and 210°C. Two methods were used for data acquisition:

1) Ascending frequency sweeps, where the frequency was increased from 0.1 to 200 rad/s at the three different temperatures.

2) Descending frequency sweeps, where the frequency was decreased from 200 to 0.1 rad/s at the three different temperatures (six frequency sweeps per sample).

Each frequency sweep was performed 2 min after the chamber reached the working temperature (170, 190, and 210°C) and the storage modulus (G′), loss modulus (G″) and complex viscosity (η*) vs angular frequency (ωx) were reported. The results of the six frequency sweeps from each sample and the principle of time-temperature superposition (TTS) were used to generate the master curves, which were calculated at a reference temperature of 170°C.

The time-temperature superposition principle was used to study the behavior of materials in a wide range of frequencies and/or temperatures. This principle transfers the information obtained to a single reference temperature, thus it is possible to compare the results from the different temperatures of all samples. The superposition principle is valid only when all relaxation times $a_\tau(T)$, in the Maxwell equation have the same temperature dependence; mathematically, this principle can be expressed as (Morgan & Harris, 2004; Zhao *et al*., 2005; Ghaffarpour & Khodaii, 2009):

$$G'(\omega, T_r) = \frac{\rho(T_r)T_r}{\rho(T)T} G'(a_\tau \omega, T) \quad (1)$$

$$G''(\omega, T_r) = \frac{\rho(T_r)T_r}{\rho(T)T} G''(a_\tau \omega, T) \quad (2)$$

where

r = reference temperature
a_τ = relation between two relaxation times at two temperatures
ρ(T) = density of the polymer at a temperature T

Results and discussion

Purification and silanization of the palygorskite

The purification of the palygorskite focused on the removal of stony waste and organic matter, and also promoted the ion exchange of calcium per sodium; the palygorskite collected from a mine naturally contains some contaminants which adversely affect the silanization process and therefore the compatibility with the thermoplastic matrix.

Figure 1 shows the FTIR spectra from the various steps of the palygorskite purification process. The absorption bands at 3700–3200 cm^{-1} correspond to the stretch vibrations of structural OH and OH of the bound and hygroscopic waters. The absorption band at 1700–1600 cm^{-1} is attributed to the bend vibration from the hygroscopic, adsorbed and bound water or from structural OH. The bands between 1300 and 400 cm^{-1} are a combination of the stretch and bend vibrations of the Si or Al–O and octahedral M–OH (M represents metal element). Table 3 lists the band positions corresponding to the functional groups of the palygorskite (Madejová & Komadel, 2001; Cai *et al*., 2007; Cheng *et al*., 2011).

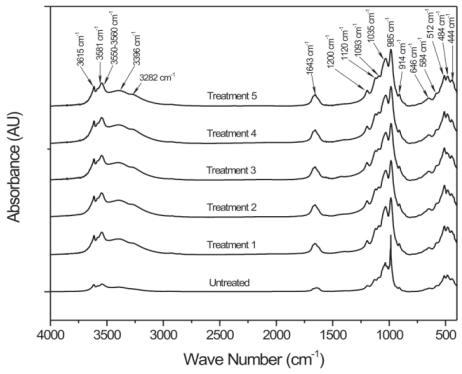

Figure 1. FTIR spectra of the different treatments from the palygorskite purification process

DOI: https://doi.org/10.1016/j.riit.2015.09.002

Table 3. FTIR band position for the palygorskite

Position (cm^{-1})	Assignation
3615	Al_2-OH
3581	Mg_2-OH
3578	Al,Fe^{3+}-OH
3551	Mg,Fe^{3+}-OH
3395	Si(OH)Si
3283	Si(OH)Al
1655	OH_2
1635	H_2O
1200	Si_U-O-Si_D
1120	Si-O
1093	Si-O
1035	Si-O
985	Si-O
914	Al_2-OH
646	Si-O
584	Si-O
512	Octahedral deformation
484	Si-O (parallel to layer)
444	MgO_6 (Rotation)

The FTIR spectra from the different treatments of the purification process show no changes compared to the spectrum from untreated palygorskite. The only differences were observed at 1655 and 1635 cm^{-1}, which correspond to water due to the hydrophilic nature of palygorskite. The spectrum from treatment 2 shows some difference at 1650 and 900 cm^{-1} which corresponds to the bending vibration mode of the hygroscopic water and Si–O structures; however, subsequent treatments show no difference at all. The bands identified in Figure 1 are similar to those reported by Cai *et al*. in their FTIR study of palygorskite (2007), the palygorskite did not show any chemical damage related to the purification process.

Figure 2 compares the FTIR spectra of purified/silanized palygorskite and purified palygorskite. The spectrum of the clay after silanization with 3-aminopropyltrimetoxysilane shows some differences in the regions corresponding to the silane, which proves silane grafting to the palygorskite (after the silanization process, the palygorskite was heavily washed with alcohol). Table 4 shows the band positions of the purified/silanized palygorskite (Madejová & Komadel, 2001).

Table 4. FTIR bands from the purified/silanized palygorskite

Position (cm^{-1})	Assignation
3615	Stretch Mg—OH dioctahedral
3516	Stretch OH of coordinated water with Al, Mg
3390	Stretch OH of zeolitic and absorbed water
3212	Stretch N—H
3050	Stretch N—H de amino (—NH_3^+)
2930	Stretch C—H
1625	Deformation OH of water
1500	Symmetric deformation N—H of amino (—NH_3^+)
1470	Deformation C—H
1194	Stretch Si–O

The bands at 3212 cm^{-1} could be assigned to the N—H stretching from the silane, the vibration at 1608 cm^{-1} also belongs to a silane amine group and it is overlapped with the 1628 cm^{-1} band characteristic of the absorbed water in the palygorskite; finally, the band at 1500 cm^{-1} corresponds to the absorption of an amino group which is absent in the palygorskite spectrum. When the palygorskite reacted with the silane, the band intensity of 2930 cm^{-1} assigned to the C—H stretching was increased due to the contribution from the organic portion of silane (Wang *et al*., 2014). In addition, the broad band at 3050 cm^{-1} corresponds to the vibrations of the $–NH_3^+$ groups from the silane (Jag & Condrate, 1972; Rozenberg & Shoham, 2007).

Microscopy analysis of the palygorskite

SEM analysis was carried out on six different samples: palygorskite without treatment (as mined) and five palygorskite samples from each treatment of the purification process. Figure 3a clearly shows the fibrillar morphology of the palygorskite without treatment at 20,000x. Figures 3b to 3e show the treated nanofibers, their morphology, length and diameter seem to be similar to the untreated fiber. However, Figure 3f shows nanofibers with substantial length reduction; apparently, the last treatment of the purification process damaged the palygorskite, probably because this treatment involves a long period of centrifugation (60 min) and sonication (60 min).

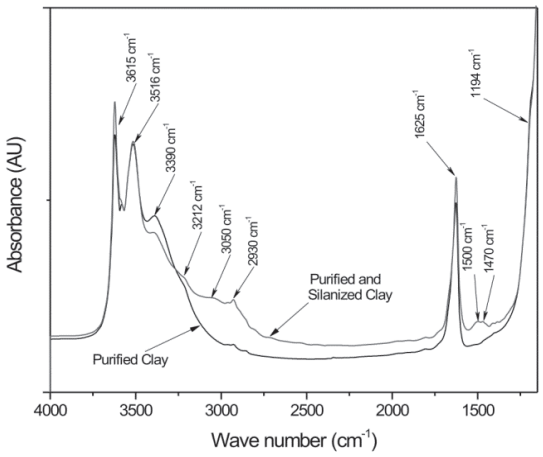

Figure 2. FTIR spectra from the palygorskite silanized with 3-aminopropyltrimetoxysilane

DOI: https://doi.org/10.1016/j.riit.2015.09.002

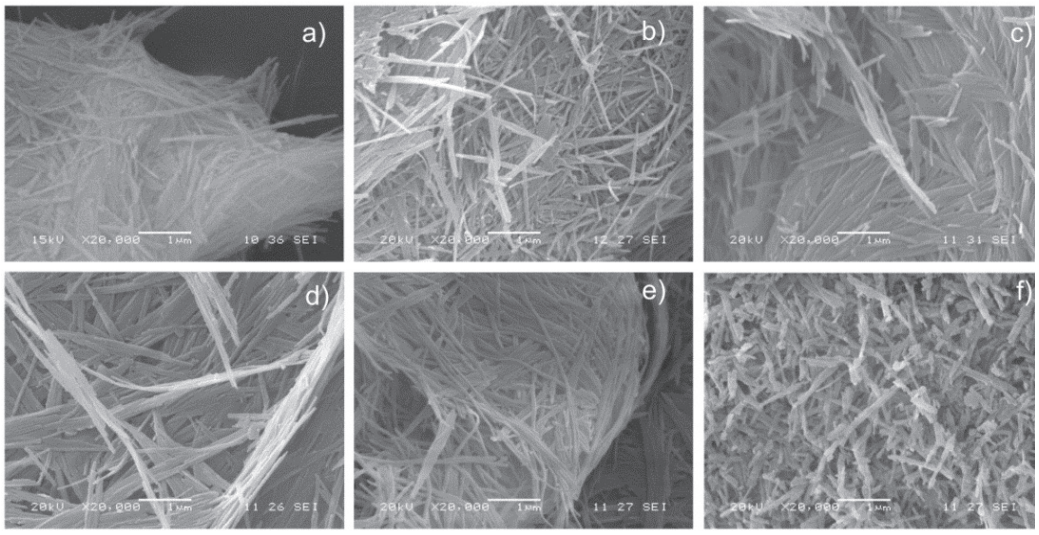

Figure 3. SEM micrographs of the palygorskite without treatment and after the five treatments of the purification process, a) without treatment, b) treatment: 1. Distiller water, c) treatment: 2. Hydrogen peroxide, d) treatment: 3. Sodium acetate, e) treatment: 4. Hydroxylamine chloride, f) treatment: 5. Sodium hexametaphosphate

Rheology analysis of the PP/MaPP/ Palygorskite formulations

The rheology properties of five different samples were measured: PP, a mixture of PP and MaPP and three formulations containing palygorskite with different chemical treatments (Table 5).

The master curves of the PP frequency sweeps are shown in Figure 4; a long relaxation time $\tau = (1/\omega_x) = (0.06868 \pm 0.0045$ s) was observed, corresponding to the frequency interval where the G′ and G″ intersect ($\omega_x = 14.56 \pm 1.02$ rad/s). Some frequency curves showed a small fluctuation of the data acquired at low frequencies; this was probably caused by the low torque signal which is near the resolution limit of the rheometer.

Figure 5 shows the rheological behavior of the mixture PP/MaPP; the relaxation time corresponding to the intersection of G′ and G″ was $\omega_x = 15.85 \pm 0.39$ rad/s is $\tau = 0.06309 \pm 0.0015$ s. This intersection interval is shorter than that of PP. The loss modulus, storage modulus and complex viscosity at high frequencies of the mixture PP/MaPP are similar to those from PP (figure 4); which is to be expected since the mixture PP/MaPP contains only 10 wt% of MaPP (with 0.6% by weight of grafted maleic anhydride), therefore, the rheological behavior is dominated by the PP.

Table 5. Samples for the rheology test; the formulations were prepared by twin-screw extrusion

Formulation	PP (wt%)	MaPP (wt%)	Palygorskite (wt%)
PP	100	0	0
PP/MaPP	90	10	0
PP/MaPP/ UC	89.5	10	0.5 (Unpurified Clay)
PP/MaPP/PC	89.5	10	0.5 (Purified Clay)
PP/MaPP/ PSC	89.5	10	0.5 (Purified and Silanized Clay)

Based on the results from Table 6, it can be said that all the formulations initially showed a similar linear behavior, since in all cases the G′, G″ and η*, slopes are similar, but the frequency interval in which G′ and G″ curve intersect is different for each formulation.

The rheological pattern of the PP/MaPP/UC formulation (Figure 6) is similar to PP, this could be caused by the low palygorskite content used (0.5 % by weight), as postulated by Zhao *et al*. (2005) "The number of particles per unit volume is a key factor in establishing the characteristic rheological response of clay nanocompo-

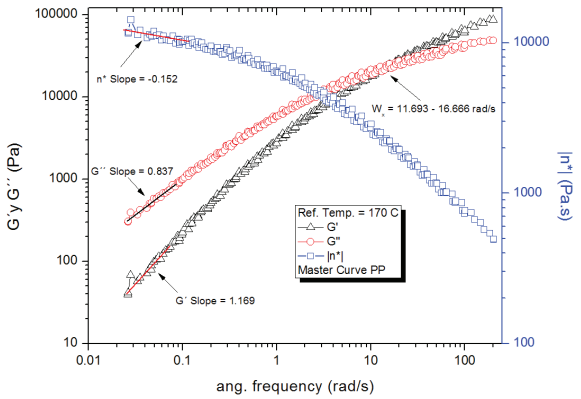

Figure 4. PP master curve from the frequency sweeps: 0.1 to 200 and 200 to 0.1 rad/s at 170, 190 and 210°C. Reference temperature 170°C

DOI: https://doi.org/10.1016/j.riit.2015.09.002

sites". In addition, the palygorskite used did not receive any surface treatment, therefore, the palygorskite particles did not fully disperse, and consequently did not substantially contribute to the strengthening of the nanocomposite.

The rheological properties of the PP/MaPP/PC and PP/MaPP/PSC mixtures showed considerable differences when compared to PP. The PP/MaPP/PC (Figure 7) showed a decrease of G′, G″ and η* both at high and low frequencies; this could be a result from the damage caused to the nanofibers of the palygorskite during the purification process (Figure 3) affecting their reinforcement ability due to the reduction of the fiber aspect ratio.

In contrast, PP/MaPP/PSC (Figure 8) showed a substantial increase of G′, G″ and η*, both at high and low frequency; although the fibers from the purified palygorskite had a reduced aspect ratio, the silanization process added functional groups to the fiber surface resulting in a better interfacial compatibility between the matrix and the reinforcement. The amino groups grafted onto the surface of the palygorskite provided a chemical bond to the polymeric matrix; accordingly with Demjén *et al*. (1999), it is believed that during the extrusion process parcial thermal degradation of the PP/MaPP generates active carboxylic groups, which may chemically react with the amino groups of the grafted silane, providing covalent links between the palygorskite and the polymer matrix, and therefore, the relaxation time of the composite is increased.

Figure 9 shows the relaxation times from each sample (Table 6); the relaxation times of the first three samples show no substantial changes; however, the last two samples show a considerable change. PSNs with purified palygorskite had a small relaxation time, consequently, the system became less elastic, resulting in a low matrix/reinforcement interaction, while the reinforcing particles created areas of stress concentrations which affected the rheological properties; most likely caused by the damage suffered by the palygorskite du-

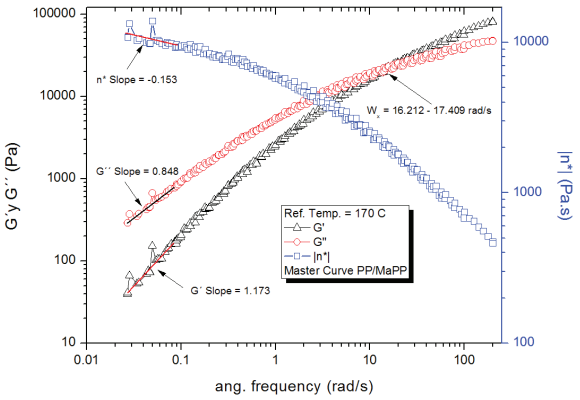

Figure 5. PP/MaPP master curve from the frequency sweeps: 0.1 to 200 and 200 to 0.1 rad/s at 170, 190 and 210°C. Reference temperature of 170°C

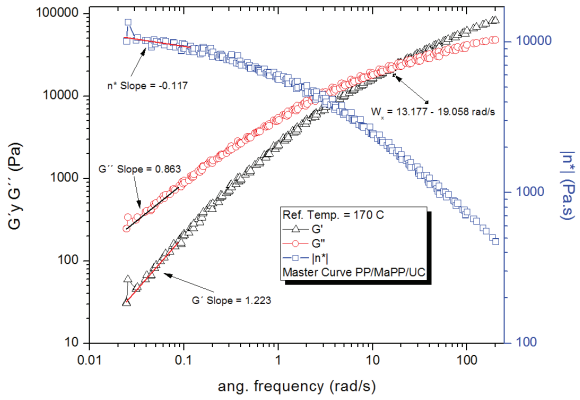

Figure 6. PP/MaPP/UC master curve from the frequency sweeps: 0.1 to 200 and 200 to 0.1 rad/s at 170, 190 and 210°C. Reference temperature of 170°C

Table 6. Summary of the rheological properties from the five different samples studied

Properties		SAMPLE PP	PP/MaPP	PP/MaPP/UC	PP/MaPP/PC	PP/MaPP/PSC
Intersection interval W_x (rad/s)		14.56±1.02	15.85±0.39	15.14±0.60	36.03±5.06	11.40±0.78
Slope Low freq.	G′	1.17	1.17	1.22	1.28	1.18
	G″	0.84	0.85	0.86	0.88	0.85
	η*	-0.15	-0.15	-0.12	-0.12	-0.14
High freq.	G′ (Pa)	86340.37	81450.98	82969.69	51861.50	102606.69
	G″ (Pa)	49049.31	47776.72	48402.53	37018.50	54267.88
	η* (Pa. S)	498.03	460.28	471.98	319.87	537.60
Low freq.	G′ (Pa)	40.19	41.37	30.34	14.54	49.55
	G″ (Pa)	308.76	301.99	254.37	144.89	335.81
	η* (Pa. S)	12174.49	11488.99	10808.26	5337.88	14138.63

DOI: https://doi.org/10.1016/j.riit.2015.09.002

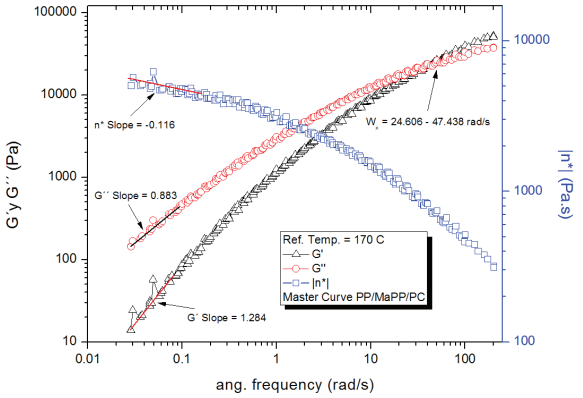

Figure 7. PP/MaPP/PC master curve from the frequency sweeps: 0.1 to 200 and 200 to 0.1 rad/s at 170, 190 y 210°C. Reference temperature of 170°C

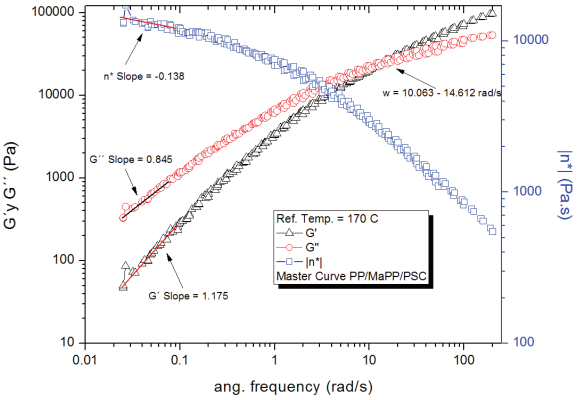

Figure 8. PP/MaPP/PSC master curve from the frequency sweeps: 0.1 to 200 and 200 to 0.1 rad/s at 170, 190 and 210°C. Reference temperature of 170°C

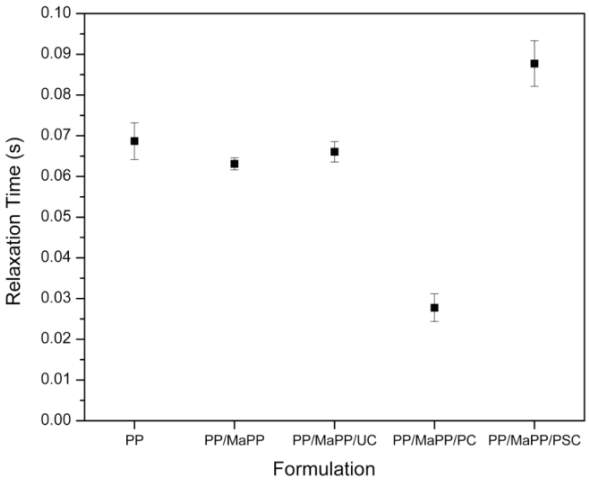

Figure 9. Relaxation times of the five formulations studied

ring the purification process. The PSNs prepared with purified and silanized palygorskite became more elastic; this formulation reported the longest relaxation time, which proves the existence of an interaction between matrix and reinforcement and therefore an improvement of the rheological properties of PSNs.

Conclusions

The infrared spectrum of purified palygorskite is consistent with the spectrum of palygorskite reported in the literature. The palygorskite's chemical structure was not affected by the extraction and purification processes.

The silanization method designed was able to chemically attach the 3-aminopropyltrimethoxysilane to the nanofiber surface, as demonstrated by the infrared spectra. The presence of silane improved the interface between the palygorskite and the polypropylene, influencing the rheological properties of the composite when melted.

SEM micrographs proved that the last treatment of the purification process, involving sodium hexametaphosphate, centrifugation and sonication, caused a morphological change in the palygorskite: the aspect ratio was reduced.

The formulation PP/MaPP/PC prepared with purified palygorskite reported the lowest values of storage modulus, probably caused by the low reinforcement content (0.5 wt%) and the damage caused to the palygorskite during the last treatment of the purification process. However, PSNs with purified/silanized palygorskite (PP/MaPP/PSC) improved their rheological properties compared to PP, despite the damage suffered by the palygorskite during the purification process.

Acknowledgment

Acknowledgment is given to Santiago Duarte Aranda for technical assistance on SEM analysis.

References

Abdul-Latif N. & Weaver C.E. Kinetic of acid-dissolution of palygorskite (attapulgite) and sepiolite. *Clay and Clay Minerals*, volume 17 (issue 3), January 1969: 169-178.

Bonilla J.L., López-González J. de D., Ramírez-Sáenz A., Rodríguez-Reinoso F., Valenzuela-Calahorro C. Activation of a sepiolite with dilute solutions of HNO_3, and subsequent heat treatment: II. Determination of surface acid centres. *Clay Minerals*, volume 16 (issue 2), September 1981:173-179.

Cai Y., Xue J., Polya D.A. A fourier transform infrared spectroscopic study of Mg-rich, Mg-poor and acid leached palygorski-

DOI: https://doi.org/10.1016/j.riit.2015.09.002

tes, Spectrochimica Acta Part A. *Molecular and Biomolecular Spectroscopy*, volume 66 (issue 2), February 2007: 282-288.

Chen J., Jin Y., Qian Y., Hu T. A new approach to efficiently disperse aggregated palygorskite into single crystal via adding freeze process into traditional extrusion treatment. *IEEE Transaction on Nanotechnology*, volume 9 (issue 1), January 2010: 6-10.

Cheng H., Yang J., Frost R.L., Wu Z. Infrared transmission and emission spectroscopic study of selected chinese palygorskites. Part A. *Spectrochimica Acta*, volume 83 (issue 1), August 2011: 518-524.

Corma A., Mifsud A., Sanz E. Influence of the chemical composition and textural characteristics of palygorskite on the acid leaching of octahedral cations. *Clay Minerals*, volume 22 (issue 2), June 1987: 225-232.

Corma A., Mifsud A., Sanz E. Kinetics of the acid leaching of palygorskite; influence of the octahedral sheet composition. *Clay Minerals*, volume 25 (issue 2), June 1990: 197-205.

Demjén Z., Pukánszky B., Nagy J. Possible coupling reactions of functional silanes and polypropylene. *Polymer*, volume 40 (issue 7), March 1999: 1763-1773.

Dos Santos-Soares D., Santana-Fernandes C., S.Da Costa A.C., Nervo-Raffin F., Acchar W., De Lima-eMoura T.F.A. Characterization of palygorskite clay from Piauí, Brazil and its potential use as excipient for solid dosage forms containing anti-tuberculosis drugs. *J. Therm Anal Calorim*, volume 113 (issue 1), June 2013: 551-558.

Duan J., Shao S., Jiang L., Li y., Jing P., Liu B. Nano-attapulguite funcionalization by silane modification for preparation of covalently-integrated epoxy/TMPTMA nanocomposites. *Iranian Polymer Journal*, volume 20 (issue 11), September 2011: 855-872.

Furuichi N., Kurokawa Y., Fujita K., Oya A., Yasuda H., Kiso M. Preparation and properties of polypropylene reinforced by smectite. *Journal of Materials Science*, volume 31 (issue 16), August 1996: 4307-4310.

Ghaffarpour-Jahromi S. & Khodaii A. Effects of nanoclay on rheological properties of bitumen binder. *Construction and Building Materials*, volume 23 (issue 8), March 2009: 2894-2904.

Gonzalez F., Pesquera C., Blanco C., Benito I., Mendioroz S., Pajares J.A. Structural and textural evolution under thermal treatment of natural and acid-activated Al-rich and Mg-rich palygorskites. *Applied Clay Science*, volume 5 (issue 1), May 1990: 23-36.

Hasegawa N., Kawasumi M., Kato M., Usuki A.,Okada A. Preparation and mechanical properties of polypropylene-clay hybrids using a maleic anhydride-modified polypropylene oligomer. *Journal of Applied Polymer Science*, volume 67 (issue 1), January 1998: 87-92.

Hasegawa N., Okamoto H., Kato M., Usuki A. Preparation and mechanical properties of polypropylene–clay hybrids based on modified polypropylene and organophilic clay. *Journal of Applied Polymer Science*, volume 78 (issue 11), December 2000: 1918-1922.

Hoffmann B., Dietrich C., Thomann R., Friedrich C., Mülhaupt R. Morphology and rheology of polystyrene nanocomposites based upon organoclay. *Macromolecular Rapid Communications*, volume 21 (issue 1), January 2000: 57-61.

Jang S.D. & Condrate R.A. The I.R. Spectra of Lysine Adsorbed on Several Caution-Substituted Montmorillonites. *Clay and Clay Minerals*, volume 20 (issue 2), April 1972: 79-82.

Jiménez-López A., López-González J. de D., Ramírez-Sáenz A., Rodríguez-Reinoso F., Valenzuela-Calahorro C., Zurita-Herrera L. Evolution of surface area in a sepiolite as a function of acid and heat treatments. *Clay Minerals*, volume 13 (issue 4), December 1978: 375-385.

Jin M. & Zhong Q. Transglutaminase cross-linking to enhance elastic properties of soy protein hydrogels with intercalated montmorillonite nanoclay. *Journal of Food Engineering*, volume 115 (issue 1), March 2013: 33-40.

Kato M., Usuki A., Okada A. Synthesis of polypropylene oligomer-clay intercalation compounds. *Journal of Applied Polymer Science*, volume 66 (issue 9), November 1997: 1781-1785.

Kawasumi M., Hasegawa N., Kato M., Usuki A., Okada A. Preparation and mechanical properties of polypropylene-clay hybrids. *Macromolecules*, volume 30 (issue 20), October 1997: 6333-6338.

Kojima Y., Usuki A., Kawasumi M., Okada A., Fukushima Y., Kurauchi T., Kamigaito O. Mechanical properties of nylon 6-clay hybrid. *Journal of Materials Research*, volume 8 (issue 5), May 1993: 1185-1189.

Koo C.M., Kim J.H., Wang K.H., Chung I.J. Melt-Extensional Properties and Orientation Behaviors of Polypropylene-Layered Silicate Nanocomposites. *Journal of Polymer Science*: Part B: Polymer Physics, volume 43 (issue 2), January 2005: 158-167.

Koo C.M., Kim M.J., Choi M.H., Kim S.O., Chung I.J. Mechanical and rheological properties of the maleated polypropylene–layered silicate nanocomposites with different morphology. *Journal of Applied Polymer Science*, volume 88 (issue 6), May 2003: 1526-1535.

Krishnamoorti R., Vaia R.A., Giannelis E.P. Structure and Dynamics of Polymer-Layered Silicate Nanocomposites. *Chemistry of Materials*, volume 8 (issue 8), August 1996: 1728-1734.

Lim Y.T. & Park O.O. Phase morphology and rheological behavior of polymer/layered silicate nanocomposites. *Rheologica Acta*, volume 40 (issue 3), May 2001: 220-229.

Madejová J. & Komadel P. Baseline of the Clay Minerals Society Source Clays: Infrared Methods. *Clays and Clay Minerals*, volume 49 (issue 5), October 2001: 410-432.

Mahi H. & Rodrigue D. Linear and non-linear viscoelastic properties of ethylene vinyl acetate/nano-crystalline cellulose composites. *Rheologica Acta*, volume 51 (issue 2), February 2012: 127-142.

DOI: https://doi.org/10.1016/j.riit.2015.09.002

Morgan A.B. & Harris J.D. Exfoliated polystyrene-clay nanocomposites synthesized by solvent blending with sonication. *Polymer*, volume 45 (issue 26), December 2004: 8695-8703.

Murray H.H. & Zhou H. Palygorskite and Sepiolite (Hormites) en: Kogel J.E., Trivedi N.C., Barker J.M., Krukowski S.T. *Industrial Minerals and Rocks*, 7th ed., New York, Society for Mining, Metallurgy, and Exploration, 2006, chapter 23, pp. 401-406.

Pesquera C., González F., Benito I., Blanco C., Mendioroz S., Pajares J.A. Passivation of a montmorillonite by the silica created in acid activation. *Journal of Materials Chemistry*, volume 2 (issue 9), September 1992: 907-911.

Reichert P., Nitz H., Klinke S., Brandsch R., Thomann R., Mülhaupt R. Poly (propylene)/organoclay nanocomposite formation: Influence of compatibilizer functionality and organoclay modification. *Macromolecular Materials and Engineering*, volume 275 (issue 1), February 2000: 8-17.

Rozenberg M. & Shoham G. FTIR spectra of solid poly-l-lysine in the stretching NH mode range. *Biophysical Chemistry*, volume 125 (issue 1), January 2007: 166-171.

Soberanis G. *Propiedades reológicas en fundido de materiales compuestos termoplásticos reforzados con nanoarcilla de paligorskita,* (tesis doctorado en ciencia), Mérida Yucatán, Centro de Investigación Científica de Yucatán, 2015, 156 pp.

Tessier A., Campbell P.G.C. & Bisson M. Sequential extraction procedure for the speciation of particulate trace metals. *Analytical Chemistry*, volume 51 (issue 7), June 1979: 844-851.

Vaia R.A., Sauer B.B., Tse O.K., Giannelis E.P. Relaxations of confined chains in polymer nanocomposites: Glass transition properties of poly (ethylene oxide) intercalated in montmorillonite. *Journal of Polymer Science*, Part B: Polymer Physics, volume 35 (issue 1), January 1997: 59-67.

Vaia R.A. & Giannelis E.P. Polymer Melt Intercalation in Organically-Modified Layered Silicates: Model Predictions and Experiment. *Macromolecules*, volume 30 (issue 25), December 1997: 8000-8009.

Ville J., Médéric P., Huitric J., Aubry T. Structural and rheological investigation of interphase in polyethylene/polyamide/nanoclay ternary blends. *Polymer*, volume 53 (issue 8), February 2012: 1733-1740.

Wang K.H., Xu M., Choi Y.S., Chung I.J. Effect of aspect ratio of clay on melt extensional process of maleated polyethylene/clay nanocomposites. *Polymer Bulletin*, volume 46 (issue 6), July 2001: 499-505.

Wang C., Ding L., Wu Q., Liu F., Wei J., Lu R., Xie H., Cheng R. Soy polyol-based polyurethane modified by raw silylated palygorskite. *Industrial Crops and Products*, volume 57 (issue 1), March 2014: 29-34.

Zhao J., Morgan A.B., Harris J.D. Rheological characterization of polystyrene–clay nanocomposites to compare the degree of exfoliation and dispersion. *Polymer*, volume 46 (issue 20), September 2005: 8641-8660.

Citation for this article:

Chicago citation style

Soberanis-Monforte, Genaro Antonio, José Luis Gordillo-Rubio, Pedro Iván González-Chi. Influence of chemically treated palygorskite over the rheological behavior of polypropylene nanocomposites. Ingeniería Investigación y Tecnología, XVI, 04 (2015): 491-501.

ISO 690 citation style

Soberanis-Monforte G.A., Gordillo-Rubio J.L., González-Chi P.I. Influence of chemically treated palygorskite over the rheological behavior of polypropylene nanocomposites. *Ingeniería Investigación y Tecnología,* volume XVI (issue 4), October-December 2015: 491-501.

About the authors

Genaro Antonio Soberanis-Monforte. PhD student on science of polymeric materials from Centro de Investigación Científica de Yucatán, A.C., master degree on polymeric materials from Centro de Investigación Científica de Yucatán, A.C., mechanical engineering from Instituto Tecnológico de Mérida. Certified engineer on leakage tests by PEMEX gas station franchise, Lechurer of the Universidad Tecnológica Metropolitana, of the Universidad Marista de Mérida and the Universidad Autónoma de Yucatán.

Pedro Iván González-Chi. PhD on polymer science and technology from Manchester Materials Science Centre/UMIST. MSc. on polymer science and technology from Manchester Materials Science Centre/UMIST. Industrial chemical engineering from Universidad Autónoma de Yucatán. Working experience: 1998 to 2000: associate researcher, Centro de Investigación Científica de Yucatán, A.C., 2001 to date, titular researcher. Centro de Investigación Científica de Yucatán, A.C., 2009 to date, Head of the Materials Department. Centro de Investigación Científica de Yucatán, A.C.

José Luis Gordillo-Rubio, Industrial chemist from the Chemical Engineering School of the Universidad Autónoma de Yucatán. Master science on polymeric materials from Centro de Investigación Científica de Yucatán, A.C. Certified chemist on the analysis of superpave asphalt by the Mexican Institute of Transport.